ISSN 1070-3284, Russian Journal of Coordination Chemistry, 2017, Vol. 43, No. 10, pp. 693–699. © Pleiades Publishing, Ltd., 2017.

Synthesis, Characterization, Crystal Structures, and Antibacterial Activity of Polynuclear Nickel(II) and Copper(II) Complexes with Similar Tridentate Schiff Bases[1]

W. H. Sun[a], K. H. Li[a], H. Liu[b], Y. T. Gu[b], Y. Zhang[b], Z. L. You[b], and W. Li[a, c, *]

[a] *Department of Radiology, The Second Hospital of Dalian Medical University, Dalian, 116023 P.R. China*

[b] *Department of Chemistry and Chemical Engineering, Liaoning Normal University, Dalian, 116029 P.R. China*

[c] *Department of Hepatobiliary and Pancreatic Surgery, The Second Hospital of Dalian Medical University, Dalian, 116023 P.R. China*

**e-mail: liwei_dlmu@126.com*

Received January 18, 2017

Abstract—An end-on azido-bridged dinuclear nickel(II) complex $[Ni_2(L^1)_2(\mu_{1,1}\text{-}N_3)_2] \cdot CH_3COOH$ (**I**) and an end-on azido-bridged polynuclear copper(II) complex $[CuL^2(\mu_{1,1}\text{-}N_3)]_n$, where L^1 is the deprotonated form of 2-[(2-ethylaminoethylimino)methyl]-4-fluorophenol and L^2 is the deprotonated form of 2-[(2-dimethylaminoethylimino)methyl]-4-fluorophenol, were prepared and characterized by elemental analysis and FT-IR spectra. Crystal and molecular structures of the complexes were determined by single crystal X-ray diffraction method (CIF files CCDC nos. 942641 (**I**) and 942642 (**II**)). Single crystal X-ray structural studies indicate that the Schiff base ligands coordinate to the metal atoms through phenolate oxygen, imine nitrogen, and amine nitrogen. The Ni atoms in the nickel complex are in octahedral coordination, and the Cu atoms in the copper complex are in square pyramidal coordination. Crystals of the complexes are stabilized by hydrogen bonds. The Schiff bases and the complexes showed potent antibacterial activities.

Keywords: nickel complex, copper complex, Schiff base, crystal structure, hydrogen bonding, antibacterial activity

DOI: 10.1134/S1070328417100104

INTRODUCTION

Polymeric structures of complexes with bridging groups are currently attracting much attention for their interesting structures and wide applications [1–4]. Schiff bases derived from salicylaldehyde and its derivatives are kinds of versatile ligands in coordination chemistry. The rational design and construction of polymeric structures of complexes with Schiff bases are of particular interest in coordination and structural chemistry. The preferred way to construct polynuclear complexes is the use of suitable bridging groups, such as N_3^-, NCS^-, $N(CN)_2^-$, dicarboxylate, 4,4'-Bipy, and so on [4–7]. Among the bridging groups, azido ligand has been attracted most attention because of its diversity of coordination modes with metal atoms, such as $\mu_{1,1}$ (end-on, EO), $\mu_{1,3}$ (end-to-end, EE), $\mu_{1,1,3}$, $\mu_{1,1,1}$, $\mu_{1,1,1,1}$, $\mu_{1,1,3,3}$, etc. [8–10]. Even though a great number of Schiff bases and their complexes have been reported in recent years, very few complexes with Schiff bases derived from 5-fluorosalicylaldehyde have been reported so far. Moreover, no complexes have been prepared from 2-[(2-ethylaminoethylimino)methyl]-4-fluorophenol (**HL[1]**) and 2-[(2-dimethylaminoethylimino)methyl]-4-fluorophenol (**HL[2]**) (Scheme 1). Considering the introduction of fluoro-substituent groups to the Schiff bases may bring novel properties such as biological activities [11]. In the present work, an end-on azido-bridged dinuclear nickel(II) complex $[Ni_2(L^1)_2(\mu_{1,1}\text{-}N_3)_2] \cdot CH_3COOH$ (**I**) and an end-on azido-bridged polynuclear copper(II) complex $[CuL^2(\mu_{1,1}\text{-}N_3)]_n$ (**II**) were prepared and characterized. The preliminary antibacterial activities have been investigated.

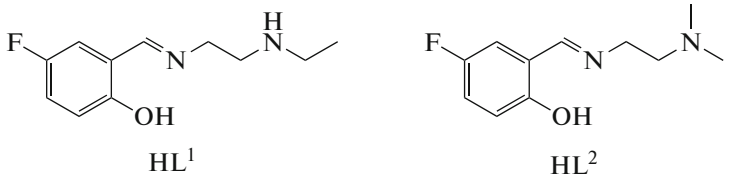

HL^1 HL^2

Scheme 1.

[1] The article is published in the original.

EXPERIMENTAL

Materials and measurements. Commercially available 5-fluorosalicylaldehyde, *N*-ethylethane-1,2-diamine and *N*,*N*-dimethylethane-1,2-diamine were purchased from Aldrich and used without further purification. Other solvents and reagents were made in China and used as received. Elemental analyses (C, H and N) were performed with a Perkin-Elmer elemental analyser. Infrared spectra were recorded on a Nicolet AVATAR 360 spectrometer as KBr pellets in the 4000–400 cm^{-1} region.

Synthesis of HL^1 and HL^2. 5-Fluorosalicylaldehyde (1.0 mmol, 0.14 g) with *N*-ethylethane-1,2-diamine and *N*,*N*-dimethylethane-1,2-diamine (1.0 mmol, 0.088 g), respectively, were dissolved in methanol (30 mL) with stirring. The mixtures were stirred for about 30 min at room temperature to give yellow solution. The solvent was evaporated to give yellow gummy products of HL^1 and HL^2, which were used for the preparation of complexes without purification.

Synthesis of complex I. A methanolic solution (10 mL) of nickel acetate tetrahydrate (0.1 mmol, 24.9 mg) was added to a methanolic solution (10 mL) of HL^1 (0.1 mmol, 21.0 mg) and sodium azide (0.1 mmol, 6.5 mg) with stirring. The mixture was stirred for 30 min to give a green solution. The resulting solution was allowed to stand in air for a few days. Green block-shaped crystals suitable for X-ray single crystal analysis were formed at the bottom of the vessel. The isolated product was washed three times with cold methanol and dried in a vacuum over anhydrous $CaCl_2$. The yield was 37%.

For $C_{28}H_{44}N_{10}F_2O_8Ni_2$

Anal. calcd., %:	C, 41.8;	H, 5.5;	N, 17.4.
Found, %:	C, 41.6;	H, 5.6;	N, 17.5.

Synthesis of complex II. A methanolic solution (10 mL) of copper chloride dihydrate (0.1 mmol, 17.5 mg) was added to an acetonitrile solution (10 mL) of HL^2 (0.1 mmol, 21.0 mg) and sodium azide (0.1 mmol, 6.5 mg) with stirring. The mixture was stirred for 30 min to give a blue solution. The resulting solution was allowed to stand in air for a few days. Blue block-shaped crystals suitable for X-ray single crystal analysis were formed at the bottom of the vessel. The isolated product was washed three times with cold methanol, and dried in a vacuum over anhydrous $CaCl_2$. The yield was 53%.

For $C_{11}H_{14}N_5FOCu$

Anal. calcd., %:	C, 42.0;	H, 4.5;	N, 22.2.
Found, %:	C, 41.9;	H, 4.4;	N, 22.4.

X-ray structure determination. Diffraction intensities for the complexes were collected at 298(2) K using a Bruker D8 Venture Photon diffractometer with MoK_α radiation (λ = 0.71073 Å). The collected data were reduced using the SAINT program [12] and multi-scan absorption corrections were performed using the SADABS program [13]. The structures were solved by direct methods and refined against F^2 by full-matrix least-squares methods using the SHELXTL [14]. All of the nonhydrogen atoms were refined anisotropically. H atoms were placed in idealized positions and constrained to ride on their parent atoms. The crystallographic data for the complexes are summarized in Table 1. Selected bond lengths and angles are given in Table 2.

Supplementary material for structures has been deposited with the Cambridge Crystallographic Data Centre (CCDC nos. 942641 (**I**) and 942642 (**II**); deposit@ccdc.cam.ac.uk or http://www.ccdc.cam.ac.uk).

Antibacterial tests. 1.5 cm^3 of a 24-h broth culture containing approximately 10^6 Cfu/cm^3 was placed in sterile petri-dishes. Molten nutrient agar (20 cm^3) kept at ~45°C was then poured in the petri-dishes and allowed to solidify. Then 2 holes of 6 mm diameter were punched carefully using a sterile cork borer and these were completely filled with the test solutions (5000 μg cm^{-3} in DMSO). The mean value obtained for the two holes was used to calculate the zone of growth inhibition of each sample.

Determination of MIC (minimum inhibitation concentration) was done using the serial dilutions in liquid broth method. The materials used were 96-well plates, suspensions of microorganism (0.5 McFarland), Muller-Hinton broth (Merck) and stock solutions of each substance to be tested (5000 μg cm^{-3} in DMSO). The following concentrations of the substances to be tested were obtained in the 96-well plates: 2500, 1250, 625, 312, 156, 78, 39, 20, 10 and 5 μg cm^{-3}. After incubation at 37°C for 18–24 h, the MIC for each tested substance was determined by microscopic observation of microbial growth. It corresponds to the well with the lowest concentration of the tested substance where microbial growth was clearly inhibited.

RESULTS AND DISCUSSION

The molecular structure and atom numbering scheme of complex **I** is shown in Fig. 1a. The asymmetric unit of the complex contains a centrosymmetric end-on azido-bridged dinuclear nickel(II) complex and two acetic acid molecules. The inversion center is located at the midpoint of the two Ni atoms. The Ni···Ni separation is 3.240(1) Å. The Schiff bases serve as tridentate ligands to form five- and six-membered chelate rings with Ni atoms in the complex. The coordination geometry around the metal center can be best described as a slight distorted octahedron with the three donor atoms of the Schiff base ligand and one

Table 1. Crystallographic data and refinement parameters for complexes **I** and **II**

Parameter	Value	
	I	**II**
Mr	804.1	314.8
Crystal color, habit	Green, block	Blue, block
Crystal size, mm	0.32 × 0.30 × 0.27	0.30 × 0.27 × 0.26
Crystal system	Monoclinic	Orthorhombic
Space group	$P2_1/n$	*Pbca*
Unit cell parameters:		
a, Å	11.801(2)	19.549(2)
b, Å	10.691(1)	6.6457(5)
c, Å	15.102(2)	19.903(2)
β, deg	111.147(2)	90
V, Å^3	1776.9(4)	2585.8(3)
Z	2	8
ρ_{calcd}, g cm^{-3}	1.503	1.617
μ, mm^{-1}	1.131	1.701
F(000)	840	1288
Number of unique data	3063	2646
Number of observed data ($I > 2\sigma(I)$)	1802	2235
Independent parameters	230	174
Number of restraints	0	0
R_1, wR_2 ($I > 2\sigma(I)$)	0.0906, 0.2143	0.0303, 0.0723
R_1, wR_2 (all data)	0.1597, 0.2657	0.0404, 0.0776
Goodness of fit on F^2	1.052	1.140
Largest difference peak and hole, *e* Å^{-3}	0.871 and –0.580	0.298 and –0.190

azido N atom defining the equatorial plane and with the symmetry-related azido N atom and one methanol O atom occupying the two axial positions. The Ni atom in the complex lies 0.073(2) Å from the least-squares plane of the equatorial donor atoms, in the direction of the methanol ligand. The bond distances and bond angles in the complex are typical and are comparable to those observed in nickel(II) complexes with Schiff bases [15, 16].

In the crystal structure of complex **I** (Fig. 2a), the acetic acid molecules are linked to the complex species through intermolecular O–H···O and N–H···O hydrogen bonds (Table 3).

The molecular structure and atom numbering scheme of complex **II** is shown in Fig. 1b. The adjacent Cu···Cu distance is 4.189(2) Å. The smallest repeat unit of the complex contains one [$CuL^2(N_3)$] moiety. The Schiff bases serve as tridentate ligands to form five- and six-membered chelate rings with Cu atoms in the complex. The coordination geometry around the metal center can be best described as a slight distorted square pyramid with the three donor atoms of the Schiff base ligand and one azido N atom defining the basal plane and with the symmetry-related azido N atom occupying the apical position. The Cu atom in the complex lies 0.080(2) Å from the least-squares plane of the basal donor atoms, in the direction of the apical donor atom. The bond distances and bond angles in the complex are typical, and are comparable to those observed in copper(II) complexes with Schiff bases [17–19].

In the crystal structure of complex **II** (Fig. 2b), molecules are linked through intermolecular C–H···O/N hydrogen bonds (Table 3), forming a 3D network.

The IR spectra of the free Schiff bases and the complexes provide information about metal–ligand bonding. The assignments are based on typical group frequencies. Weak and sharp absorptions at 3200–3300 cm^{-1} for the Schiff bases and complex I can be assigned to ν(N–H). The intense absorption at 2087 cm^{-1} for **I** and 2049 cm^{-1} for **II** are assigned to the stretching vibrations of azide ligands. Strong absorptions centered at 1639 cm^{-1} in spectra of the free

Table 2. Selected bond distances (Å) and angles (deg) for complexes **I** and **II***

Bond	*d*, Å	Bond	*d*, Å
		I	
Ni(1)–N(1)	1.996(7)	Ni(1)–N(2)	2.121(7)
Ni(1)–N(3)	2.082(7)	Ni(1)–O(1)	2.048(6)
Ni(1)–O(2)	2.129(6)	Ni(1)–N(3*A*)	2.145(7)
		II	
Cu(1)–O(1)	1.9099(15)	Cu(1)–N(1)	1.9510(17)
Cu(1)–N(2)	2.0851(18)	Cu(1)–N(3)	1.9996(19)
Cu(1)–N(3*A*)	2.611(2)		
Angle	ω, deg	Angle	ω, deg
		I	
N(1)Ni(1)O(1)	91.0(3)	N(1)Ni(1)N(3)	172.8(3)
O(1)Ni(1)N(3)	91.4(3)	N(1)Ni(1)N(2)	83.6(3)
O(1)Ni(1)N(2)	174.5(3)	N(3)Ni(1)N(2)	93.9(3)
N(1)Ni(1)O(2)	95.4(3)	O(1)Ni(1)O(2)	87.3(3)
N(3)Ni(1)O(2)	91.5(3)	N(2)Ni(1)O(2)	94.3(3)
N(1)Ni(1)N(3*A*)	93.2(3)	O(1)Ni(1)N(3A)	91.5(3)
N(3)Ni(1)N(3*A*)	79.9(3)	N(2)Ni(1)N(3A)	87.7(3)
O(2)Ni(1)N(3*A*)	171.3(3)		
		II	
O(1)Cu(1)N(1)	93.20(7)	O(1)Cu(1)N(3)	89.26(7)
N(1)Cu(1)N(3)	170.92(8)	O(1)Cu(1)N(2)	177.28(6)
N(1)Cu(1)N(2)	84.10(7)	N(3)Cu(1)N(2)	93.36(7)
O(1)Cu(1)N(3A)	87.77(7)	N(1)Cu(1)N(3A)	90.90(7)
N(2)Cu(1)N(3A)	92.61(7)	N(3)Cu(1)N(3A)	97.93(7)

* Symmetry codes: (*A*) $1-x, 1-y, -z$ (**I**); (*A*) $2-x, 1/2+y, 1/2-z$ (**II**).

Table 3. Geometrical parameters of hydrogen bonds for complexes **I** and **II***

D–H···A	Distance, Å			Angle D–H···A, deg
	D–H	H···A	D···A	
		I		
O(3)–H(3)···O(1)$^{\#1}$	0.82	1.79	2.569(11)	158
N(2)–H(2*A*)···O(1)$^{\#2}$	0.91	2.51	3.351(9)	155
		II		
C(6)–H(6)···N(5)$^{\#3}$	0.93	2.49	3.356(7)	154
C(10)–H(10*C*)···O(1)$^{\#4}$	0.96	2.39	3.319(7)	162
C(11)–H(11*C*)···O(1)$^{\#5}$	0.96	2.57	3.523(7)	176

* Symmetry codes: $^{\#1}$ $x, y, 1+z$; $^{\#2}$ $1-x, 1-y, -z$; $^{\#3}$ $x, 3/2-y, -1/2+z$; $^{\#4}$ $2-x, 1/2+y, 1/2-z$; $^{\#5}$ $2-x, -1/2+y, 1/2-z$.

Schiff bases are assigned to azomethine, ν(C=N), which shift to lower wavenumbers in the complexes 1623 cm^{-1} for **I** and 1626 cm^{-1} for **II**. The shift indicates coordination of the azomethine N to metal. In both complexes, the Schiff base ligand coordination to the metal atoms is also substantiated by weak bands at low wavenumbers.

The zone of inhibition for the 5000 μg cm^{-3} test solutions (DMSO as the solvent) on the four bacteria: *Escherichia coli*, *Pseudomonas aeruginosa*, *Salmonella*

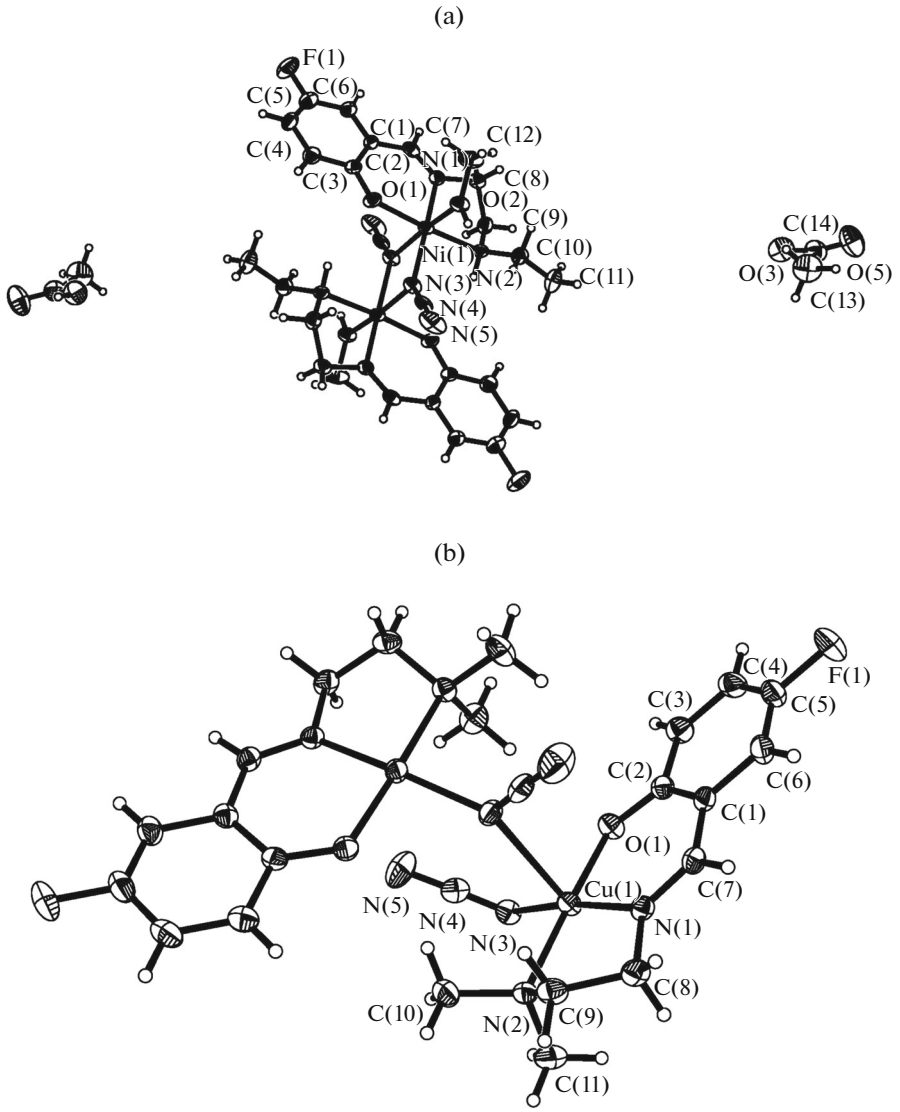

Fig. 1. ORTEP plot of the crystal structures of **I** (a) and **II** (b). Displacement ellipsoids of non-hydrogen atoms are drawn at the 30% probability level. Unlabeled atoms are at the symmetry positions $1 - x$, $1 - y$, $- z$ (for **I**) and $2 - x$, $1/2 + y$, $1/2 - z$ (for **II**).

typhi and *Staphylococcus aureus* is given in Table 4. The MIC values are given in Table 5. The results indicated that there was no obvious activity observed by the Schiff bases against *E. coli* and *S. aureus*, except for the weak inhibition to *P. aeruginosa* and *S. typhi*, whereas the two complexes had obvious inhibition on the culture of the four bacteria. It is noteworthy that the zones of inhibition areas are somewhat larger for the complexes than the ligands. The trend in this work is accord with those reported earlier [20, 21], which have shown that metal complexes are more potent bactericidal than that of the corresponding Schiff bases. This is probably due to the greater lipophilic nature of the complexes. Such increased activity of the metal chelates can be explained on the basis of chelating theory [22]. On chelating, the polarity of the metal ion will be reduced to a greater extent due to the overlap of the ligand orbital and partial sharing of positive charge of the metal ion with donor groups. Further, it increases the delocalization of π-electrons over the whole chelate ring and enhances the lipophilicity of the complex. This increased lipophilicity enhances the penetration of the complexes into lipid membrane and blocks the metal binding sites on enzymes of microorganisms [23].

Thus, an end-on azido-bridged dinuclear nickel(II) complex and an end-on azido-bridged polynuclear copper(II) complex derived from Schiff bases 2-[(2-ethylaminoethylimino)methyl]-4-fluorophenol and 2-[(2-dimethylaminoethylimino)methyl]-4-fluorophenol were prepared and characterized by elemental analysis and FT-IR spectra. The Schiff bases coordinate to the metal atoms through phenolate oxygen, imino nitrogen, and amino nitrogen. Azide

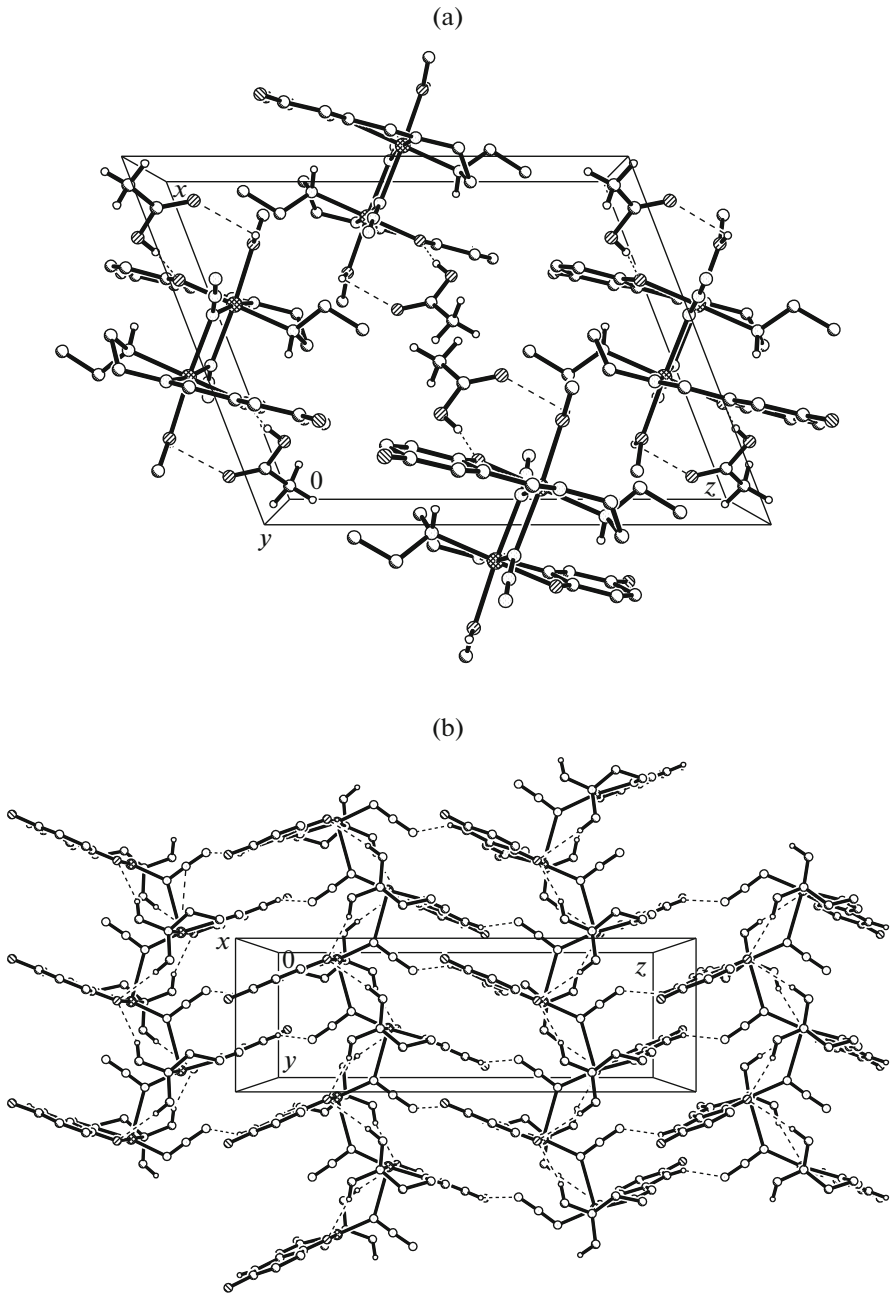

Fig. 2. Molecular packing arrangement of **I** (a) and **II** (b) displayed in the unit cell. Hydrogen bonds are shown as dashed lines.

Table 4. Antibacterial screening results

Compound	Zone of inhibition, mm			
	*E. coli**	*P. aeruginosa*	*S. typhi*	*S. aureus**
HL^1		4.5	6.1	
HL^2		5.0	6.8	
I	7.7	9.6	15.3	4.9
II	9.0	15.2	13.8	6.5

* Missing values indicates that the bacteria are resistant to the compound.

Table 5. Antibacterial activities as MIC values (μg cm^{-3})

Compound	*E. coli*	*P. aeruginosa*	*S. typhi*	*S. aureus*
HL^1		312	156	
HL^2		312	156	
I	312	78	39	156
II	78	39	10	156

ligands in the complexes adopt end-on bridging mode. The nickel and copper complexes exhibited higher antibacterial activities than the Schiff base ligands.

REFERENCES

1. Katsaros, N., Katsarou, M., Sovilj, S.P., et al., *Bioinorg. Chem. Appl.*, 2004, vol. 2, nos. 3–4, p. 193.
2. Karaliota, A., Kamariotaki, M., Hadjipanajioti, D., et al., *J. Inorg. Biochem.*, 1998, vol. 69, nos. 1–2, p. 79.
3. Liimatainen, J., Lehtonen, A., and Sillanpaa, R., *Polyhedron*, 2000, vol. 19, no. 9, p. 1133.
4. Rao, S.N., Munshi, K.N., Rao, N.N., et al., *Polyhedron*, 1999, vol. 18, no. 19, p. 2491.
5. Dinda, R., Ghosh, S., Falvello, L.R., et al., *Polyhedron*, 2006, vol. 25, no. 12, p. 2375.
6. Bagherzadeh, M., Amini, M., Parastar, H., et al., *Inorg. Chem. Commun.*, 2012, vol. 20, no. 1, p. 86.
7. Dinda, R., Sengupta, P., Ghosh, S., et al., *Dalton Trans.*, 2002, vol. 23, no. 23, p. 4434.
8. Liu, D., Zhou, Q., Chen, Y., et al., *Dalton Trans.*, 2010, vol. 39, no. 23, p. 5504.
9. Tian, C.-B., Li, Z.-H., Lin, J.-D., et al., *Eur. J. Inorg. Chem.*, 2010, no. 3, p. 427.
10. Zhou, X.-S., You, Z.-L., Xian, D.-M., et al., *Chin. J. Inorg. Chem.*, 2013, vol. 29, no. 4, p. 850.
11. Zhang, M., Xian, D.-M., Li, H.-H., et al., *Aust. J. Chem.*, 2012, vol. 65, no. 4, p. 343.
12. *SMART and SAINT*, Madison: Bruker AXS Inc., 2002.
13. Sheldrick, G.M., *SADABS, Program for Empirical Absorption Correction of Area Detector*, Göttingen: Univ. of Göttingen, 1996.
14. Sheldrick, G.M., *SHELXTL V5.1, Software Reference Manual*, Madison: Bruker AXS, Inc., 1997.
15. Sasmal, S., Hazra, S., Kundu, P., et al., *Inorg. Chem.*, 2010, vol. 49, no. 20, p. 9517.
16. Zhou, X.-S., Cheng, X.-S., Li, Y.-N., et al., *Chin. J. Inorg. Chem.*, 2013, vol. 29, no. 2, p. 397.
17. Qian, S.-S., Zhang, M., Cheng, X.-S., et al., *Synth. React. Inorg. Met.-Org. Nano-Met. Chem.*, 2013, vol. 43, no. 8, p. 1059.
18. Bhowmik, P., Jana, S., and Chattopadhyay, S., *Polyhedron*, 2012, vol. 44, no. 1, p. 11.
19. Zhang, M., Xian, D.-M., Zhang, N., et al., *Struct. Chem.*, 2012, vol. 23, no. 5, p. 1489.
20. You, Z.-L. and Jiao, Q.-Z., *Synth. React. Inorg. Met.-Org. Nano-Met. Chem.*, 2006, vol. 36, no. 10, p. 713.
21. Xue, L.-W., Zhao, G.-Q., Han, Y.-J., et al., *Synth. React. Inorg. Met.-Org. Nano-Met. Chem.*, 2011, vol. 41, no. 2, p. 141.
22. Searl, J.W., Smith, R.C., and Wyard, S., *J. Proc. Phys. Soc.*, 1961, vol. 78, no. 505, p. 1174.
23. Rosu, T., Negoiu, M., Pasculescu, S., et al., *Eur. J. Med. Chem.*, 2010, vol. 45, no. 2, p. 774.